Experimental

Cryo-TEM images were taken at the Laboratory of Materials and Interface Chemistry of Eindhoven University of Technology. Sample preparation for cryo-TEM was carried out in an automated vitrification robot (FEI Vitrobot™ Mark III) using liquid ethane as cryogen. TEM grids (Quantifoil R2/2, Quantifoil Micro Tools GmbH, Jena, Germany) were glow discharged prior to use in a Cressington 208 carbon coater for 40 seconds. Cryo samples were imaged with the TU/e CryoTitan (FEI, www.cryotem.nl). The CryoTitan is equipped with a with a field emission gun (FEG), a post column Gatan Energy Filter (GIF) and was operated at 300 kV. Images were recorded on a post-GIF 2k x 2k Gatan CCD camera using zero-loss energy filtering with a 20 eV energy window. The images in Figure 3 (3SI) and 5 (5SI) were post-processed in Matlab to increase clarity with a median filtered (3x3 kernel) to remove noise and background subtracted (median 220x220 kernel) to account for the varying ice thickness.

Cryo-electron tomography data (cryo-TEM tilt-series) were acquired with Inspect3D (FEI company) by recording cryo-TEM images (as noted above) over a tilt range of ±60˚ with 3˚ increments. For acquisition a nominal defocus of -15 µm was used and the total accumulated dose over the entire tilt-series was 80 electrons / $Å^2$. The tilt-series were processed in IMOD [J. R. Kremer, D.N. Mastronarde, J.R. McIntosh (1996) J. Struct. Biol. 116:71-76.] which included: manually supervised alignment of the images by cross-correlation, binning to a final pixel size of 1.9 nm, and reconstruction by weighted backprojection. Subsequently the reconstructions were denoised using nonlinear anistropic diffusion (k=5000,i=10) [A. Frangakis, R. Hegerl (2001) J. Struct. Biol. 135: 239-205.], corrected for inhomogeneous background by subtracting the median (kernel size=50^3) filtered volume and manually segmented in Amira 4.1 (Mercury Computer Systems). For comparison the datasets were also segmented in Matlab by thresholding and morphological filtering which gave very similar results, however, without the possibility to separate individual sheets which manual segmentation provides.

Cryo-TEM images for Figure 2 and 7 were taken with a Philips CM120 BioTWIN Cryo microscope at the National Center for High Resolution Electron Microscopy (nCHEM) at Lund University. Specimen were prepared in a controlled environment vitrification system (CIVS) (Bellare, J.R.; Davis,H. T.; Scriven, L. E.; Talmon,Y. J. ElectronMicrosc. Tech. 1988, 10, 87-111.) using a standard protocol (Talmon, Y. Ber. Bunsen Ges. Phys. Chem. 1996, 100, 364-372.).To improve the wetting properties, the grids were treated by glow discharge, which temporarily forces the hydrophobic surface of the carbon grid to become more hydrophilic. Samples were placed on the grids after glow discharge, followed by fast dipping of the grids in liquid ethane and transfer to liquid nitrogen. Grids were kept in liquid nitrogen prior to imaging.

Small-angle X-ray scattering experiments were conducted on beamline I711 at the MAX II storage ring in Lund, Sweden, using a sample-to-detector distance of 1.243 m and a wavelength of λ = 1.1 A°. The details regarding the experimental setup are explained elsewhere[35]. Samples were carefully loaded, using syringes, into quartz capillaries. In the data reduction, the decay of the intensity of the primary beam and the transmission of samples were

taken into account by measuring the beam intensity with a semiconducting diode immediately before and after sample exposure.

Computational

The mechanism of formation of A_6K type peptide nanotubes has been investigated with the semiempirical PM3 method. The large number of atoms in this system prohibits the usage of ab initio quantum mechanical approaches, semiempirical molecular orbital methods are used instead. A study on cyclo[(-L-Phe^1-D-Ala^2-)$_{n=3\text{-}6}$] and cyclo[(-L-Phe^1-D-^{Me}*N*-Ala^2-)$_{n=3\text{-}6}$] and their dimers optimized by both the semiempirical molecular orbital AM1 method and the B3LYP/6-31G* method have shown similar characteristics in structures and energies[36]. Synthetic organic functional nanomaterials have been the subject of intense study due to their potential use in many fields. Seven models of a novel photo-switchable self-organized peptide system were optimized using the semi-empirical molecular orbital method AM1[37]. In this study, PM3 is preferred over AM1 since it is known that PM3 is superior in modelling systems with hydrogen bonds[38].

The polypeptides have been drawn and optimized with PM3 in Spartan08[39] and then Gaussian 09[40] has been used to confirm the nature of the stationary points with positive vibrational frequencies calculated with the same method. The effect of a polar environment has been taken into account by the integral equation formalism polarizable continuum model (IEF-PCM)[41], with water as the solvent.

Binding electronic energies are calculated by using the equation 1:

$$E_{binding-trimer} = E_{trimer} - E_{dimer} - E_{monomer} \qquad (1)$$

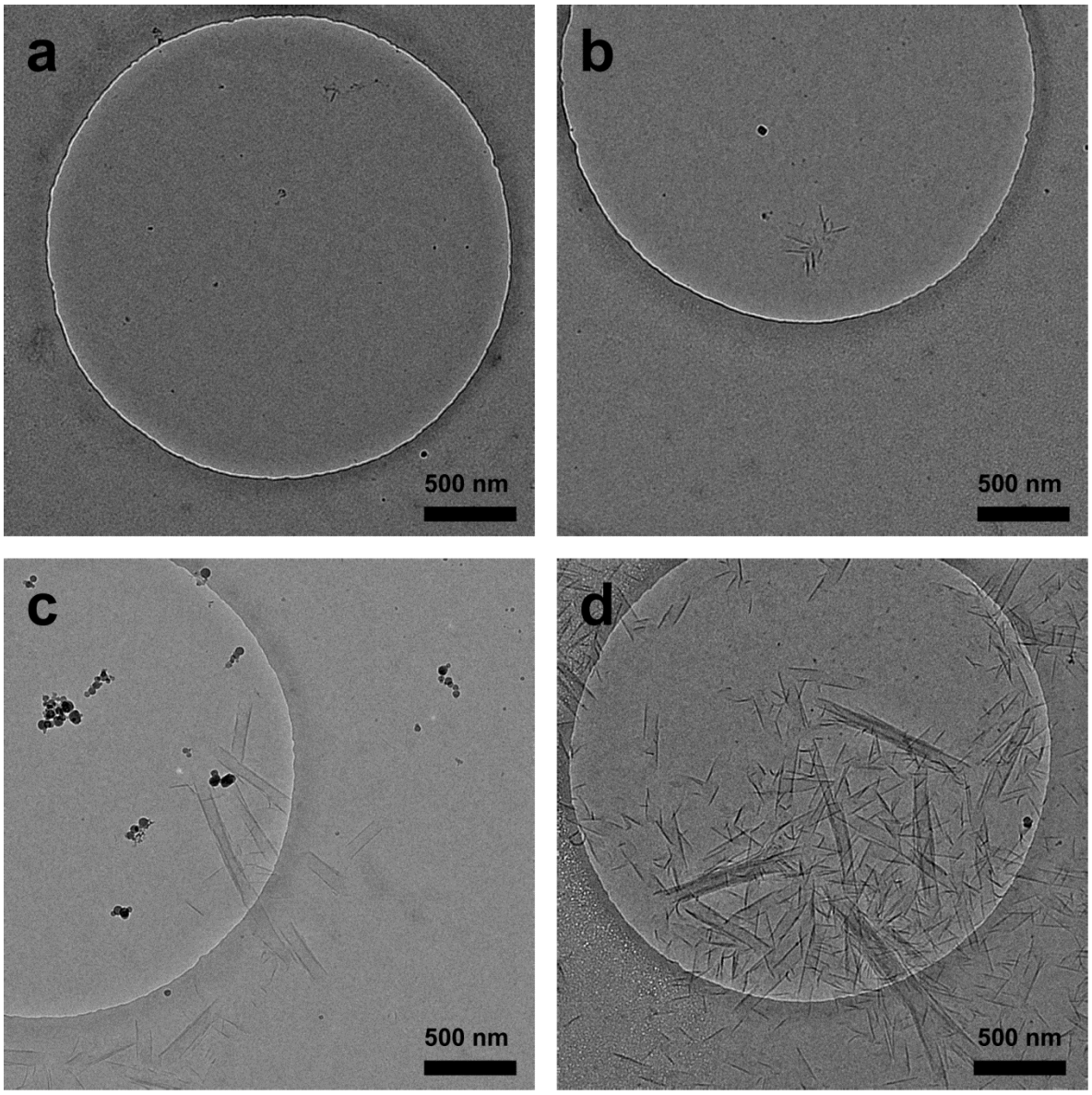

Figure SI1. Overview images of nanotube formation upon temperature quench from 70 ^{o}C to 20 ^{o}C after (a) 0 minutes (b) 15 minutes (c) 30 minutes (d) 120 minutes. The dark spots in the images, particularly panel (c), are ice contamination from ambient air. Ice contamination cannot be fully prevented as prepared cryo TEM grids are manually inserted into Titan autoloader cartridges at liquid nitrogen temperatures.

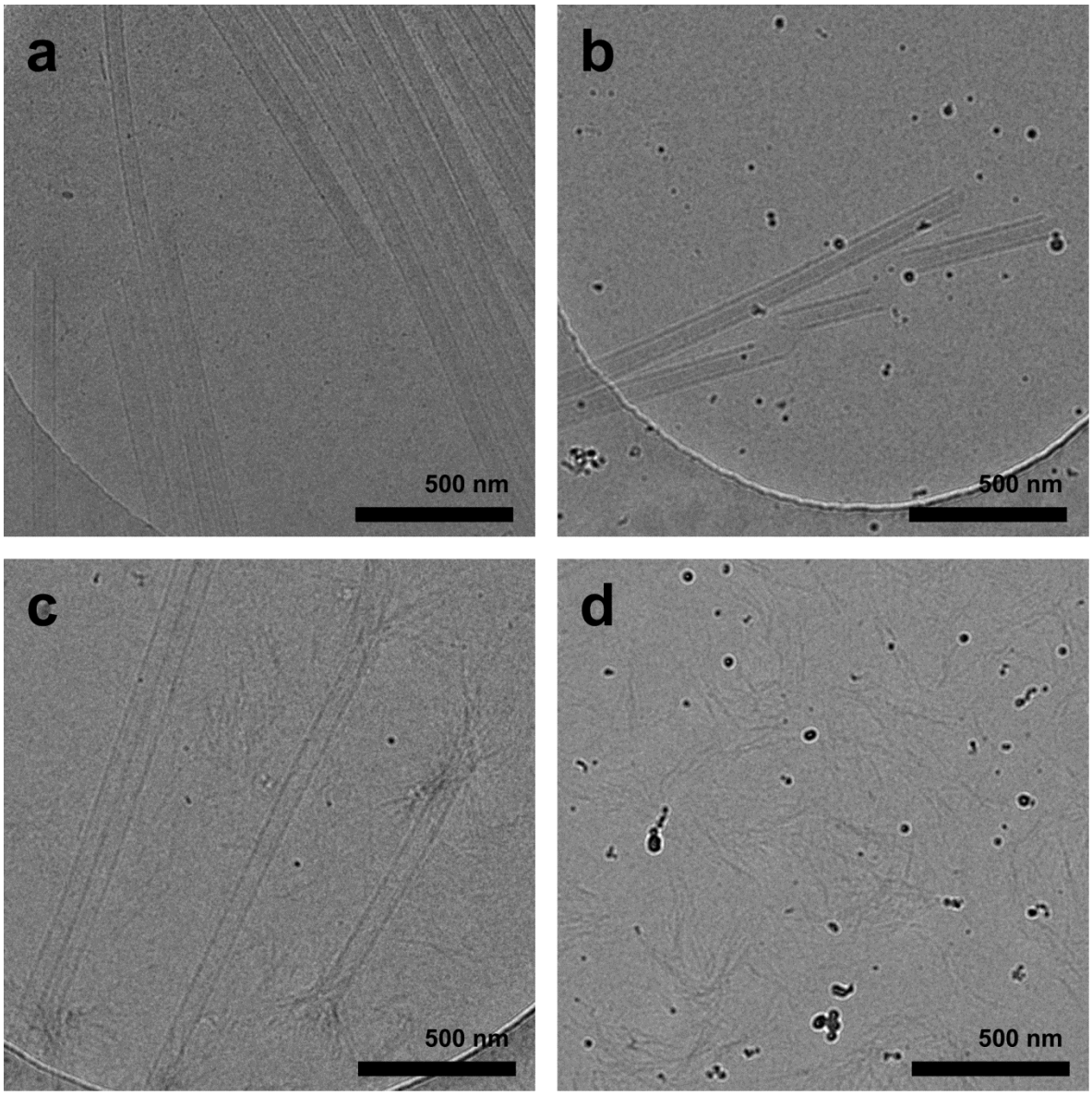

Figure SI2. Dissolution of nanotubes by heating to 70 ^{o}C and vitrification after (a) 15 seconds (b) 60 seconds (c) 120 seconds (d) 300 seconds. The dark spots in the images, particularly panel (b, d), are ice contamination from ambient air during sample transfer.

References

35 M. Knaapila, C. Svensson, J. Barauskas, M. Zackrisson, S. S. Nielsen, K. N. Toft, B. Vestergaard, L. Arleth, U. Olsson, J. S. Pedersen and Y. Cerenius, J. Synchrotron Radiat., 2009, 16, 498–504.
36 G. Chen, S. Su and R. Liu, J. Phys. Chem. B, 2002, 106, 1570–1575.
37 W. Qu, H. Tan, G. Chen and R. Liu, Phys. Chem. Chem. Phys., 2003, 5, 2327–2332.
38 S. Schr€oder, V. Daggett and P. Kollman, J. Am. Chem. Soc., 1991, 113, 8922–8925.
39 Spartan 08, Wavefunction Inc., Irvine CA, 2008.
40 M. J. Frisch, G. W. Trucks, H. B. Schlegel, G. E. Scuseria, M. A. Robb; J. R. Cheeseman, G. Scalmani, V. Barone, B. Mennucci, G. A. Petersson, H. Nakatsuji, M. Caricato, X. Li, H. P. Hratchian, A. F. Izmaylov, J. Bloino, G. Zheng, J. L. Sonnenberg, M. Hada, M. Ehara, K. Toyota, R. Fukuda, J. Hasegawa, M. Ishida, T. Nakajima, Y. Honda, O. Kitao, H. Nakai, T. Vreven, J. A. Montgomery, J. E. Peralta, F. Ogliaro, M. Bearpark, J. J. Heyd, E. Brothers, K. N. Kudin, V. N. Staroverov, J. Normand, K. Raghavachari, A. Rendell, J. C. Burant, S. S. Iyengar, J. M. Cossi, N. Rega, J. M. Millam, M. Klene, J. E. Knox, J. B. Cross, V. Bakken, C. Adam, J. Jaramillo, R. Gomperts, R. E. Stratmann, O. Yazyev, A.

J. Austin, R. Cammi, C. Pomelli, J. W. Ochterski, R. L. Martin, K. Morokuma, V. G. Zakrzewski, G. A. Voth, P. Salvador, J. J. Dannenberg, S. Dapprich, A. D. Daniels, O. Farkas, J. B. Foresman, J. V. Ortiz, J. Cioslowski and D. J. Fox, Gaussian09, Gaussian, Inc., Wallingford CT, 2009.
41 (a) J. Tomasi, B. Mennucci and E. Canc_es, THEOCHEM, 1999, 464, 211–226; (b) M. T. Canc_es, B. Mennucci and J. Tomasi, J. Chem. Phys., 1997, 107, 3032–3041; (c) B. Mennucci and J. Tomasi, J. Chem. Phys., 1997, 106, 5151–5158; (d) B. Mennucci, E. Canc_es and J. Tomasi, J. Phys. Chem. B, 1997, 101, 10506–10517.